

## Vorticity Hole Surrounding a Point Vortex

SANPEI Akio\*, KIWAMOTO Yasuhito<sup>1</sup> and ITO Kiyokazu

*Graduate School of Human and Environmental Studies, Kyoto University, Sakyo-ku, Kyoto 606-8501, Japan*

*<sup>1</sup>Faculty of Integrated Human Studies, Kyoto University, Sakyo-ku, Kyoto 606-8501, Japan*

(Received: 5 December 2000 / Accepted: 14 September 2001)

### Abstract

Depleted regions (holes) in the vorticity distribution often play a controlling role in the evolution of two-dimensional turbulence. We report experimental investigations of the generation process and the geometries of ring holes surrounding a strongly-peaked clump of vorticity (point vortex) immersed in a background of the extended vorticity distribution.

### Keywords:

electron plasma, vortex, 2-dimensional turbulence

### 1. Introduction

In the two-dimensional (2D) dynamics of an electron column immersed in a strong uniform magnetic field, the density  $n(x,y)$  and the potential distribution  $\phi(x,y)$  is equivalent to the vorticity  $\zeta(x,t)$  and stream function  $\psi(x,y)$  of 2D Euler fluid, respectively. Areas of excessive (depleted) density in the 2D plane are called clumps (holes) in the vorticity distribution. In a non-neutral plasma, because of a lack of counter-charge particles, coulomb force is partially shielded only by density depressions, i.e. formation of holes.

We have recognized the appearance of patched holes or ring holes in the early phase of our experimental studies of point vortex motion in an extended vorticity distribution. [1,2,3] Such ring holes have been introduced in a theoretical model for explaining crystallization of clumps in the perspective of statistical mechanics. [4] In the model, a major role of the ring hole appears to be a barrier against local entropy transport. There is an experiment about formation of the hole by Huang [5], and Schechter theoretically analyzed the motion of hole in an extended vortex. [6] It has been pointed out that the holes have controlling effects on the evolution of turbulence because of their relatively slow motion among clumps.

In this paper we examine the time scale of the formation process of the ring holes and characteristics of their geometries in regard with the shape and strength of the extended vortex interaction with a point vortex or clump.

The experimental data are obtained with an electron plasma confined in a Malmberg trap. The details of configuration and diagnostics have been reported elsewhere. [1,2,3,7]

### 2. Process of Hole Formation [8]

Figure 1 illustrates the dynamics of a clump injected at  $t = 10 \mu\text{sec}$  in a low vorticity region of an extended vortex. The darkness is proportional to the vorticity, and the black dot represents the clump. The peak vorticity  $\zeta_{v,0}$  of clump is about 180 times that of the extended vorticity  $\zeta_{b,0}$ , and its circulation  $\Gamma_v$  is about 0.18 times the extended vortex'  $\Gamma_b$ . The clump generates a rotational flow around its center in the same direction as that generated by the extended vortex ( $t = 20 \mu\text{sec}$ ). The interacting flows make the clump climb along the gradient  $\partial\zeta_b(r)/\partial r$  of the background vortex trailing a spiral arm of the perturbed vorticity distribution. [3] The clump drags a part of the low vorticity area into the

\*Corresponding author's e-mail: n50117@sakura.kudpc.kyoto-u.ac.jp

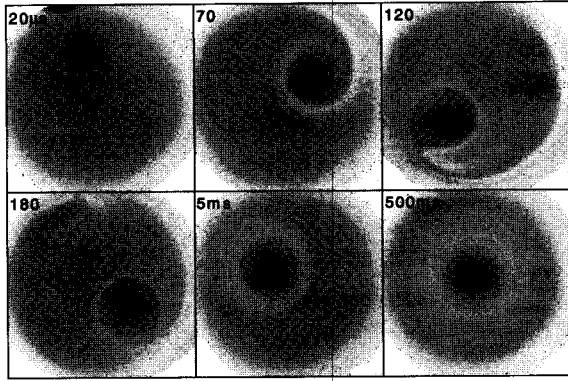


Fig. 1 Snapshots of the vorticity distribution generating a ring hole around a clump interacting with an extended vortex.

higher vorticity area of extended vortex and makes a spiral streak around its center ( $t = 70 \mu\text{sec}$ ). The differential flow around the clump shortens the distance between the spiral streaks ( $t = 120 \mu\text{sec}$ ). The spiral streaks reconnect ( $t = 180 \mu\text{sec}$ ), and negative-vorticity region involved in extended vorticity forms a ring hole that surrounds the clump ( $t = 5 \text{ msec}$ ). Once generated the ring hole has a long lifetime comparable with that of the clump ( $t = 500 \text{ msec}$ ). We examine the speed of the generation process of the ring hole in terms of the reconnection time  $T_R$  of the streak.

### 3. Empirical Scaling of Reconnection Time [8]

By injecting a clump in the periphery of an extended vortex that has various levels and slightly different gradients of vorticity as illustrated in Fig. 2, we have observed the formation process of a ring hole. The radial position of the injection is indicated by an arrow. We define  $T_R$  as the time elapsed from injection of the clump to the occurrence of reconnection of the streak circulating around it. The reconnection time intricately depends on  $\Gamma_v$  and the local condition imposed by the background distribution  $\zeta_b(r)$  of the extended vortex.

Figure 3 plots  $T_R$  against the circulation  $\Gamma_v$  of the clump for four different distributions of the extended vortex. We have empirically found that a power law holds between  $T_R$  and  $\Gamma_v$  and that the power depends on  $\beta = |\zeta_b \partial \zeta_b / \partial r|$  at the initial location of the clump. The fitting lines for the data set in Fig. 3 provide an empirical relation,  $T_R \propto (\Gamma_0 / \Gamma_v)^{(\beta_0 / \beta)^2}$ , where the fitting parameters are  $\Gamma_0 = 15 \text{ m}^2 \text{ sec}^{-1}$ , and  $\beta_0 = 8.9 \times 10^9 \text{ m}^{-1} \text{ sec}^{-2}$ .

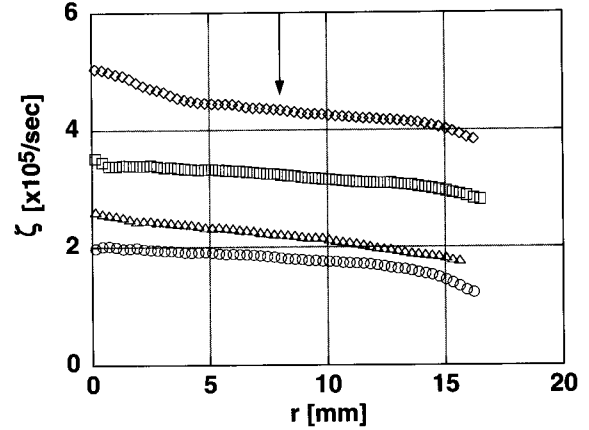


Fig. 2 Radial profiles of the extended vortex. The initial location of the clump is indicated by an arrow.

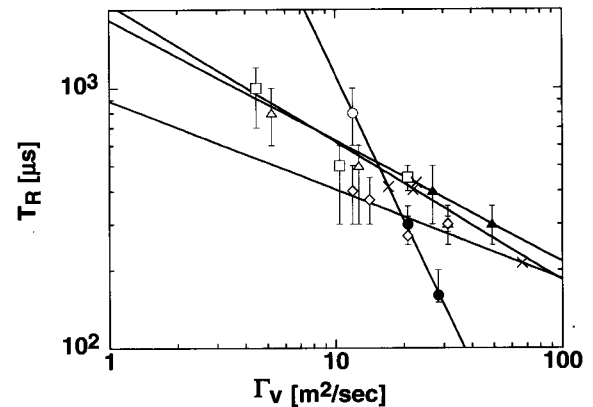


Fig. 3 Reconnection time is plotted against  $\Gamma_v$ . Each symbol corresponds to the different profiles in Fig. 2. The difference between closed and open symbols is described in relation to Fig. 5 (a).

The coefficient connecting the empirical scaling is determined by plotting the observed  $T_R$  that is divided by the right-hand-side against  $\beta$ . The final relation reads as,

$$T_R = a \left( \frac{\beta_0}{\beta} \right)^{1/2} \left( \frac{\Gamma_0}{\Gamma_v} \right)^{(\beta_0 / \beta)^2}, \quad (1)$$

where  $a = 5.2 \times 10^2 \mu\text{sec}$ . Figure 4 plots the observed values of the reconnection time  $T_{R-\text{EXP}}$  against the associated values  $T_{R-\text{CAL}}$  obtained from the empirical relation (1). It demonstrates that Eq. (1) represents the wide class of the observed data quite satisfactorily.

A recent paper by Durkin *et al.* [9] has proposed that the wave-braking time  $T_{\text{wb}} \propto \lambda^{-1} \ln \lambda^{-1}$  is a good measure of describing the reconnection time, where  $\lambda =$

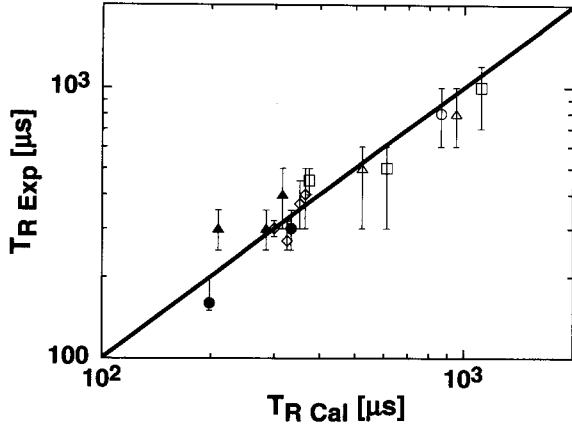


Fig. 4 The observed reconnection time is plotted against the prediction of the empirical scaling (1).

$\Gamma_v/\Gamma_b$ . We have examined the correlation between  $T_R$  obtained in our experiments and the observed  $\lambda$ , but did not obtain meaningful relation between them. Our current evaluation of this model is that it cannot be applied to the general cases with inhomogeneous background distribution though it may be valid to a special case of flat disk distribution of the extended vortex.

So far we have not obtained a full physical explanation of the relation (1). Noticing experimental data indicating a functional relation between  $\beta$  and the shear  $A = -r d\Omega_b(r)/dr$  that has global meaning, we expect that the relation will be reconstructed from a shear flow model including the contribution of the clump.

#### 4. Functional Analysis of Examination of Empirical Relation

Now we analyze what effect the profile of extended vortex has on the reconnection time. Let us set  $\gamma = \ln(\Gamma_v/\Gamma_0)$  and  $\hat{\beta} = \beta/\beta_0$ . Then the right hand side of Eq. (1) is written as

$$f(\hat{\beta}) = a \hat{\beta}^{-1/2} \exp[-\gamma/\hat{\beta}^2]. \quad (2)$$

We renormalize Eq. (2) by dividing it by its value at  $\hat{\beta}_e = 2|\gamma|^{1/2}$  to obtain

$$\tilde{f}(x) \equiv \frac{f(\hat{\beta})}{f(\hat{\beta}_e)} = x^{-1/2} \exp\left[\frac{\gamma}{4|\gamma|} (1 - 1/x^2)\right]. \quad (3)$$

Here we have introduced a new variable  $x = \hat{\beta}/\hat{\beta}_e$ . To compare the observed reconnection time  $T_R$  with Eq. (3), we define the normalized reconnection time as

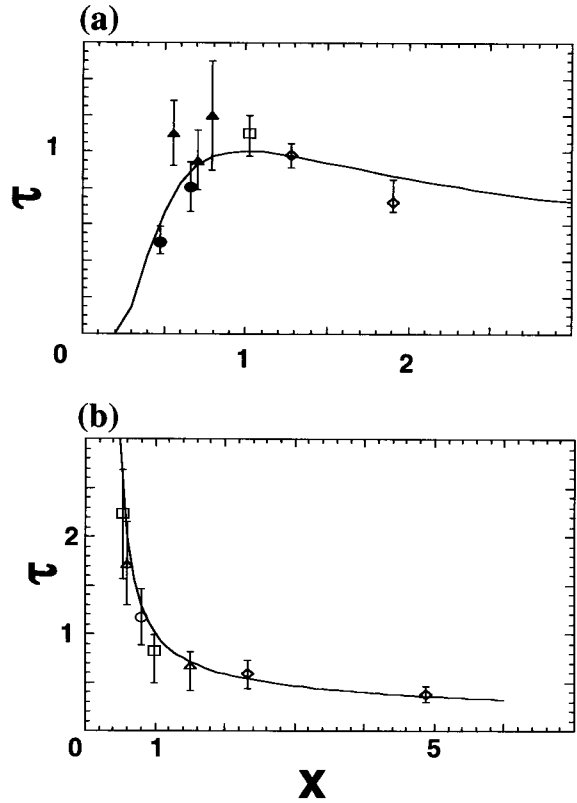


Fig. 5 Unified functional dependence of the reconnection time on  $\gamma$  and  $\beta$  is examined in the form of  $\tau = \tilde{f}(x)$ . The functional form differs depending whether  $\gamma > 0$  (a) or  $\gamma < 0$  (b).

$$\tau \equiv \frac{T_R}{f(\hat{\beta}_e)}. \quad (4)$$

The functional form of  $\tilde{f}(x)$  depends on the sign of  $\gamma$ . Figure 5 plots the function  $\tilde{f}(x)$  for  $\gamma > 0$  in (a) and for  $\gamma < 0$  in (b) in solid curve. The experimental data are plotted also in corresponding graphs. Here  $x$  and  $\tau$  are determined from the observed parameters. We can observe an excellent agreement between individual data and the unique function  $\tilde{f}(x)$  that has two branches of form appearing from a degenerated expression in Fig. 3.

The data points with  $\gamma > 0$  and  $x < 1$  are represented by closed symbols, while other data points are given by open symbols. This classification traces back to Fig. 3 and Fig. 4, and the separation point  $x = 1$  is indicated by the symbols  $\times$  on the fitting lines in Fig. 3.

When  $\gamma < 0$ , clump is weak and it causes a small perturbation in the extended vortex. This region therefore may be classified as the weak-point-vortex region. When  $\gamma > 0$  so that the strength of the clump is

not weak,  $\tilde{f}(x)$  is separated into two regions separated at  $x = 1$ . In the region of  $x > 1$ ,  $\beta > \beta_0 \ln(\Gamma_v/\Gamma_0)$  so that the dynamics is dominated by the extended vortex. On the other hand, in the region of  $x < 1$ , the effect of the clump dominates in the reconnection process as may be suggested by the locations of closed symbols in Fig. 3.

### 5. Geometry of Ring Hole

Now we report about the size of the ring holes. The radius  $R_{HO}$  of the outer edge of the ring hole depends on  $\Gamma_v$  and profile  $\zeta_b(r)$  of the extended vortex. As  $\Gamma_v$  increases,  $R_{HO}$  increases to the order of the radius of the stagnation zone  $l = (\Gamma_v/2\pi|A|)^{1/2}$ .

The maximum depth in  $\zeta_H(x,y)$  of the ring hole also depends on  $\Gamma_v$  and  $\zeta_b(r)$ . The depth  $\zeta_H(x,y)$  stands for the decrement from the unperturbed level of the extended vorticity  $\zeta_b(r)$ . Our observations indicate that the maximum  $\zeta_H$  is less than 20% of the local  $\zeta_b(r)$ , and less than 1% of the peak vorticity  $\zeta_{b0}$  of the clump. We should note that  $\zeta_H$  is much smaller than the decrement in the open spiral streak generated in the wake of a clump that can reach almost 50–100% of  $\zeta_b$ . [3]

Let us examine shielding effects that the ring hole may have by defining the circulation of the hole,  $\Gamma_H = \int dx dy \zeta_H(x,y)$ . Figure 6 plots the ratio of  $\Gamma_H$  to  $\Gamma_v$  against  $1/T_{R-CAL}$ . Here we choose  $T_{R-CAL}$  in (1) because it includes several parameters relevant to the build-up of the ring holes and could be a measure of the strength to generate the holes. Though a positive correlation may be expected between  $\Gamma_H/\Gamma_v$  and  $1/T_{R-CAL}$ , the observations lead to somewhat puzzling results. We don't have a clear physical meaning of this correlation, and need more consideration about it. For all this state of our

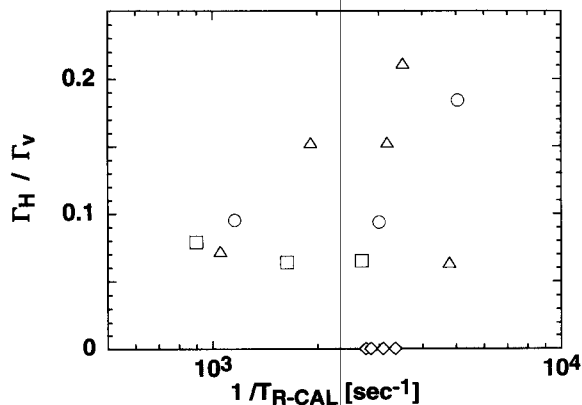


Fig. 6 The relative strength of the ring hole to the clump are plotted in terms of  $\Gamma_H/\Gamma_v$  as a function of  $1/T_R$ .

understanding, the experimental data in Fig. 6 clearly indicate that  $\Gamma_H$  lies from 5% to 20% of  $\Gamma_v$ .

This experimental evidence might raise a question to the fully-shielded vortex model in Ref. [4] and to a naive assumption of  $\Gamma_H = \Gamma_v$  introduced in Ref. [9]. Here let us note that the vortex-merging is not driven directly by the force between symmetric vortices but that merging require asymmetric deformations in the distribution of the vortices. [10] The merging drive in such a perturbational order may be effectively modified by some redistribution in the hole vorticity  $\zeta_b(x,y)$  even if  $\Gamma_H \ll \Gamma_v$ .

### 6. Conclusions

We have studied the generation process and geometrical properties of ring holes around a point vortex or clump. We have obtained an empirical scaling that includes several parameters relevant to the vortex dynamics to predict the reconnection time of a spiral streak. The geometrical properties of the ring hole indicate that the ring holes do not completely shield the clump's field. Our observations may request reconsiderations about the dynamics of interacting clumps surrounded by modified background vorticity distributions.

### Acknowledgments

The authors thank Prof. A. Mohri for stimulating discussion. This work was supported by a Grant-in-Aid from the Ministry of Education, Science, Sports and Culture and by the collaborative research program of National Institute for Fusion Science.

### References

- [1] Y. Kiwamoto, A. Mohri, K. Ito, A. Sanpei and T. Yuyama, *Non-neutral Plasma Physics III* (AIP1999) pp.99-105.
- [2] Y. Kiwamoto, K. Ito, A. Sanpei, A. Mohri, T. Yuyama and T. Michishita, *J. Phys. Soc. Jpn. (Lett.)* **68**, 3766 (1999).
- [3] Y. Kiwamoto, K. Ito, A. Sanpei and A. Mohri, *Phys. Rev. Lett.* **85**, 3173 (2000).
- [4] D.Z. Jin and D.H.E. Dubin, *Phys. Rev. Lett.* **80**, 4434 (1998).
- [5] X.-P. Huang, K.S. Fine and C.F. Driscoll, *Phys. Rev. Lett.* **74**, 4424 (1995).
- [6] D.A. Schechter and D.H.E. Dubin, *Phys. Rev. Lett.* **83**, 2191 (1999).
- [7] K. Ito, Y. Kiwamoto and A. Sanpei, *Jpn. J. Appl. Phys.* **40**, 2558 (2001).

- [8] A. Sanpei, Y. Kiwamoto and K. Ito, J. Phys. Soc. Jpn. **70**, No.10 (2001).
- [9] D. Durkin and J. Fajan, Phys. Rev. Lett. **85**, 4052 (2000).
- [10] M.V. Melander, N.J. Zabusky and J.C. McWilliams, J. Fluid Mech. **195**, 303 (1988).